Supplementary information

for

Comparing the Resilience of Macromolecular Coatings on Medical-Grade Polyurethane Foils

Maria G. Bauer[1,2], Kjetil Baglo[1,3], Luca Reichert[1,3], Jan Torgerson[1,3], Oliver Lieleg[1,2,*]

[1] School of Engineering and Design, Department of Materials Engineering, Technical University of Munich, Boltzmannstraße 15, 85748 Garching, Germany

[2] Center for Protein Assemblies and Munich Institute of Biomedical Engineering, Technical University of Munich, Ernst-Otto-Fischer Str. 8, 85748 Garching, Germany

[3] Institute of Materials Science, Technical University of Munich, Boltzmannstraße 15, 85748 Garching, Germany

*corresponding author:

Prof. Dr. Oliver Lieleg

Department of Mechanical Engineering and Munich School of Bioengineering,

Technical University of Munich, Boltzmannstraße 11, 85748 Garching, Germany

e-mail: oliver.lieleg@tum.de,

phone: +49 89 289 10952, fax: + 49 89 289 10801

SI 1 Fourier-transformed infrared spectroscopy (FTIR)

Spectra determined for uncoated and coated PCU samples are displayed in **Figure SI 1**.

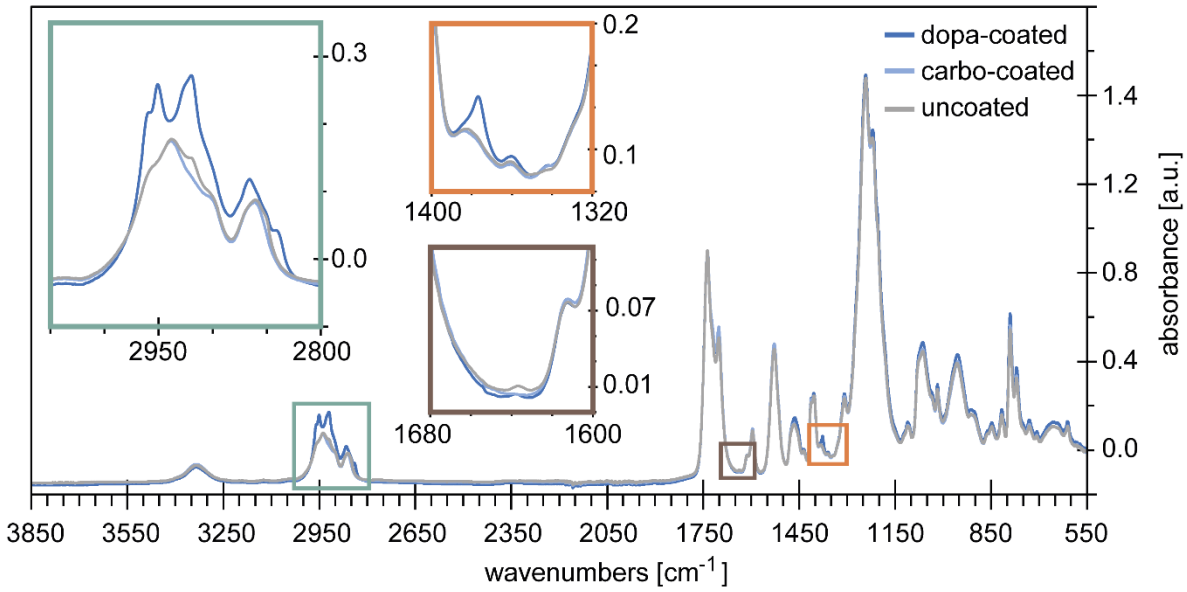

Figure SI 1: *FTIR spectra of uncoated and coated PCU samples:* Results obtained for uncoated PCU (grey), carbo-coated PCU (light blue), and dopa-coated PCU (dark blue) foils are displayed. Important ranges in the spectra are marked by the colored frames (turquoise, grey, and orange) and depicted as enlarged details in frames of the corresponding color.

Even though these FTIR spectra are – overall – rather similar, it is possible to detect some differences, especially within the following wavenumber ranges:

1) 2800 – 3050 cm^{-1} (turquoise frame),
2) 1600 – 1680 cm^{-1} (brown frame),
3) 1320 – 1440 cm^{-1} (orange frame).

The most noticeable changes in the spectra occur in the 2800 cm^{-1} to 3000 cm^{-1} range, where aliphatic hydrogen vibrations are observed. The coated samples each consist of at least three different compounds (*i.e.*, the PCU substrate, the intermediate layer, and the top-layer molecule), all of which have spectra reported in literature we can use to make comparisons with. [1–6]

For the ***uncoated PCU sample***, the highest abundance of peaks is expected for CH2 asymmetric and symmetric stretching occurring at 2938 cm^{-1} and 2862 cm^{-1}, respectively. The shoulder at 2955 cm^{-1} of medium to low intensity is likely CH_3 asymmetric stretch, with the lower intensity symmetric stretch overlapping with the CH_2 symmetric stretch. Other than these vibrations, there are peaks of medium to low abundance at 2920 cm^{-1} and 2905 cm^{-1}, which may be aliphatic vibrations from polymer additives such as plasticizers, solvents, or from certain parts of the polymer that are not accounted for by considering the functional groups. Without detailed knowledge about the synthesis and preparation of the commercial polymer material, a more detailed discussion is not possible.

For the ***dopa-coated PCU***, the spectrum shows two distinct peaks at 2920 cm^{-1} and 2950 cm^{-1} identified as CH_3 and CH_2 asymmetric stretch, with complementary symmetric vibrations at 2855 cm^{-1} and 2835 cm^{-1}. The shift to lower wavenumbers of these groups is consistent with a positively charged group such as a quaternary amine, and the peak positions correspond well with the spectra reported for quaternary amine. [6] A peak at 1377 cm^{-1} can be seen for the dopa-coated PCU sample; this peak is also strong in the spectrum of a quaternary amine and is likely to represent a CH_3 vibration mode. The lack of a similar increase in the ~1450 cm^{-1} CH_2 peak may indicate a dominant CH_3 content over CH_2 in the dopa coating – but this notion is not supported by the C-H stretching modes. It should also be noted that a C-H stretching is by no means unique to a quaternary amine and could be the result of other constituents. For instance, if the main functionalization of the surface is achieved through hydrogen bonding, then this would also show up in this range as a shift in C-H vibrations. To specifically assign the observed changes to the compositional chemistry, a more in-depth study would be needed. The primary amine band is present at 1635 cm^{-1}, but with a low abundance; the complimentary N-H stretching in the range 3450-3160 cm^{-1} is not observed, likely due to the low abundance. The secondary amine N-H stretch at 3335 cm^{-1} has a high abundance but is present for both, coated PCU films and the uncoated PCU film alike, making an evaluation difficult.

For the ***carbo-coated PCU*** sample, there is almost no change in the recorded absorbance (compared to uncoated PCU foils) except for a decrease in intensity for the peak at 2920 cm^{-1}. The lower abundance of this peak is likely due to a change in the PCU film rather than the coating, as the abundance of all other peaks remains unchanged. This change may be due to

the removal of lighter aliphatic species dissolved in the polymer network, and such a removal may occur during the atmospheric plasma treatment (@ 60 W for 25 min) and/or as a consequence of the foil exposure to highly concentrated solvents (*e.g.*, 96 % ethanol for 1 h).

Mainly, those results indicate that applying the coatings has induced minor changes to the material. For the dopa coating, the influence of the coating components is detectable in the spectra, whereas for the carbo-coating, the processing itself appears to have the greatest influence. It should be noted that FTIR tends to favor chemical groups with a strong dipole, and a more in-depth study would be required if the chemical composition of the coating and the polymer were to be described in full.

SI 2 Differential scanning calorimetry

To analyze how the applied coatings influence the heat thermal behavior, differential scanning calorimetry (DSC) scans were conducted. Therefore, a differential scanning calorimeter (DSC 300 Caliris, Netzsch Gerätebau GmbH, Selb, Germany) was employed and DSC scans were performed from -40°C to 300°C at 10°C/min. A protective flow of nitrogen at 20 ml/min was used for all measurements with sample weights of 10.2 mg, 11.3 mg, and 11.5 mg for the uncoated, dopa-, and carbo-coated samples, respectively. To fit the DSC pans, the samples were cut into squares using lab scissors and sealed in lidded aluminum pans. The heat flow recorded by DSC for the uncoated, carbo-coated, and dopa-coated PCU films are presented **Figure SI 2**.

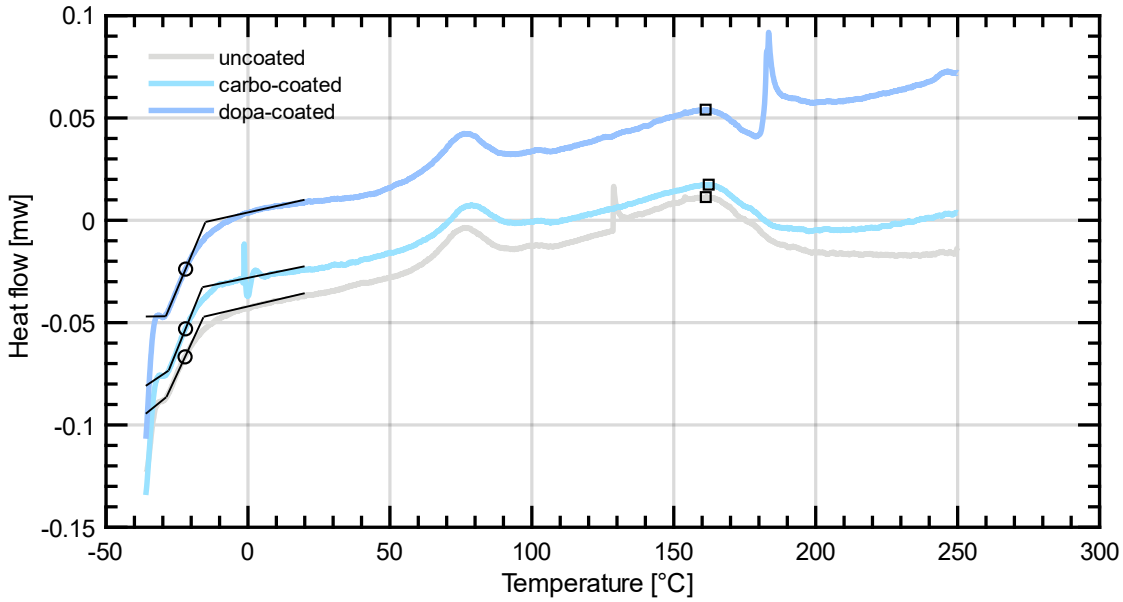

***Figure SI 2**: Influence of the coatings on the thermal behavior of the PCU foils*: The heat flow detected for temperatures ranging from -40 °C to 250 °C is displayed for uncoated (grey), carbo-coated (light blue), and dopa-coated (dark blue) PCU samples.

For all three sample types, the onset of the glass transition was estimated to be at -29 °C, while the inflection point was estimated to be at -22 °C. The melting temperature was recorded from the maximum of each broad melting peak and was determined to be 161°C for the uncoated and dopa-coated sample, and at 162°C for the carbo-coated sample. This melting temperature

is within the expected range for poly(urethane carbonates). [7] The difference between the T_g and T_m values we obtained for the uncoated PCU and the values stated by the manufacturer might be caused by different measurement conditions and/or sample dimensions/preparations. Nonetheless, especially the T_g values are still in a similar range and – more importantly – clearly below the temperature ranges used in this study.

For the carbo-coated sample, a sharp exothermic peak followed by an endothermic peak is observed around 0°C. The second feature may represent the melting of N-[3-(Trimethoxysilyl)propyl]-ethylenediamine which is reported to have a melting temperature of 0°C; and the exothermic behavior is expected for a crystalline material and is often observed for amines owing to strong hydrogen bonding. [8] Additionally, for all samples, there is an endothermic peak around 76°C followed by a slight endothermic peak at 100°C; the origin of those two peaks are most likely ethanol and water evaporation.

Overall, the DSC data suggests that the coatings do not significantly change T_g nor T_m.

SI 3 Scanning electron microscopy (SEM)

The individual interface thicknesses d_{int} derived from the acquired SEM images are listed in **Table SI 1**.

Table SI 1: *Individual interface thicknesses derived from SEM images*

$d_{int,uncoated}$ [µm]	$d_{int,carbo}$ [µm]	$d_{int,dopa}$ [µm]
0.458	0.353	1.573
0.390	0.606	1.504
0.407	0.641	0.576
0.274	0.672	1.000
0.462	0.925	0.865
0.356	0.673	0.424
0.119	0.504	0.712
0.390	1.052	1.001
0.256	0.475	1.068
0.222	0.407	4.525
0.084	0.527	5.288
	0.628	0.797
	0.477	0.763
	0.441	0.848
	0.202	1.017
	0.370	0.966
	0.289	0.949
	0.322	0.133
	1.441	0.687
	0.814	0.599
	0.678	
	0.538	
	0.404	
	0.356	
	0.441	
	0.407	

These values result in mean interface thicknesses of $\bar{d}_{int,uncoated} = (0.31 \pm 0.04)\ \mu m$, $\bar{d}_{int,carbo} = (0.56 \pm 0.05)\ \mu m$, and $\bar{d}_{int,dopa} = (1.26 \pm 0.29)\ \mu m$, respectively. The lower number of values determined for uncoated samples is caused by the fact, that the visible interface was for several images so thin, that it was not possible to reliably determine an interface thickness.

SI 4 Surface Morphologies

To compare the influence of the coatings and/or treatments on the surface morphologies of the PCU foils, profilometric images were captured as stitched collections of 3 horizontal and 4 vertical single images. To display the surface morphologies, the single images were preprocessed as described in methods section (2.6) in the manuscript; then, representative images for each coating/treatment combination were chosen and compared qualitatively to each other together with the corresponding laser microscopy images. Such morphologies are displayed for coated and long-term treated samples in **Figure SI 3,** and for coated and sterilized samples in **Figure SI 4**.

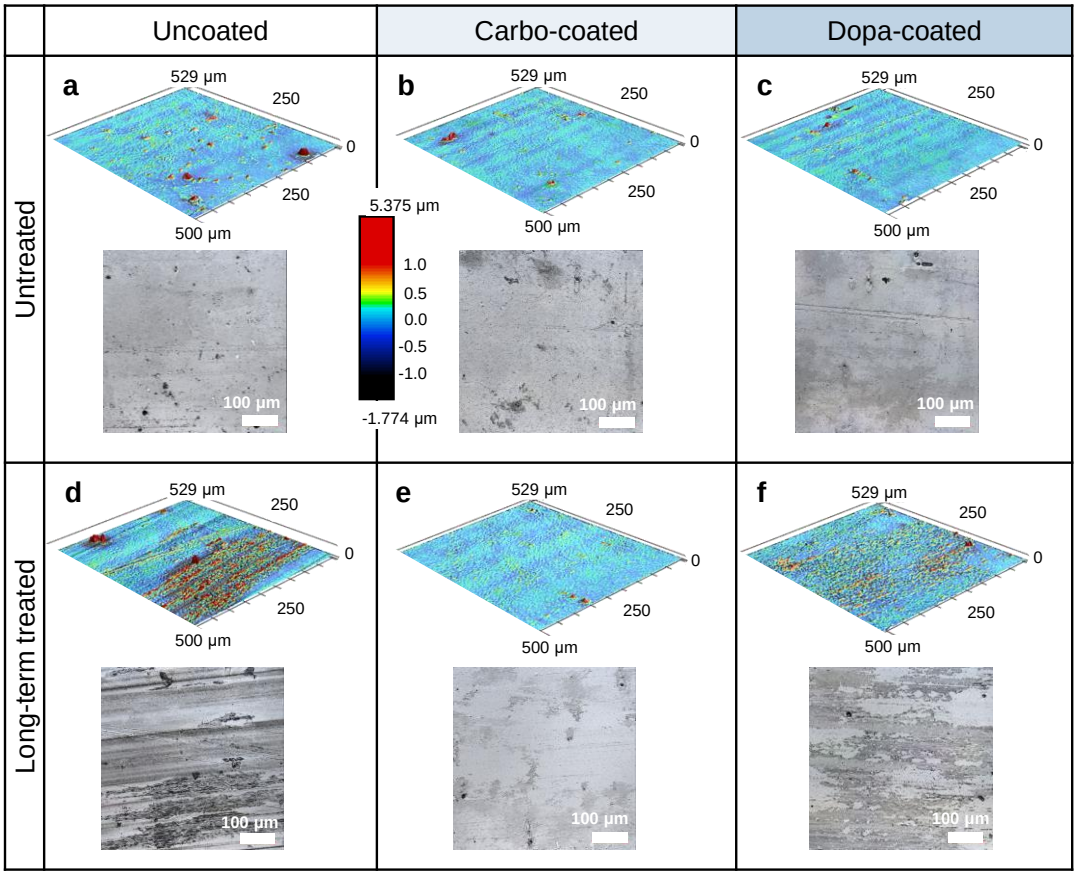

Figure SI3: *Surface morphologies and laser microscopy images of coated and long-term treated samples:* For each coating/treatment combination, a representative set of images (taken with 20x magnification) of the resulting surface structure is displayed; colored images represent height-scaled 3D surface morphologies (top pictures); grey-scale images represent laser microscopy image (bottom pictures). The color scale located between subfigures a) and b) applies to all images depicting surface morphologies.

In **Figure SI 3**, when comparing the images of the untreated samples displayed in the top row, the impression is confirmed, that neither coating appears to have a major influence on the surface morphologies of the samples. However, when each untreated sample is compared to the corresponding long-term treated sample (*i.e.*, samples exposed to 9 h of tribological load) clear differences can be observed. Whereas, on the images of the uncoated, long-term treated sample obvious grooves and valleys from the continuous linear movement are evident, almost no change is perceptible if the images associated with the carbo-coating are compared. On the images of the long-term treated, dopa-coated samples some signs of increased roughness and abrasion are visible.

If the images in **Figure SI 4** are compared with respect to the coating type, *i.e.*, column-wise, neither of the two sterilization treatments appears to have a strong influence on the surface structures or appearance of the foils when compared to each corresponding "stored" sample. Overall, the microscopy images are quite similar, and all surface morphology images can be colored using the same color scheme as their surface roughness is close to zero. However, there seems to be a small difference between the treated, uncoated samples and the control group (uncoated, untreated – only stored), which is not observable for either of the coated samples. This indicates that the applied surface coatings might help reduce putative influences the sterilization procedures have on the substrate material itself.

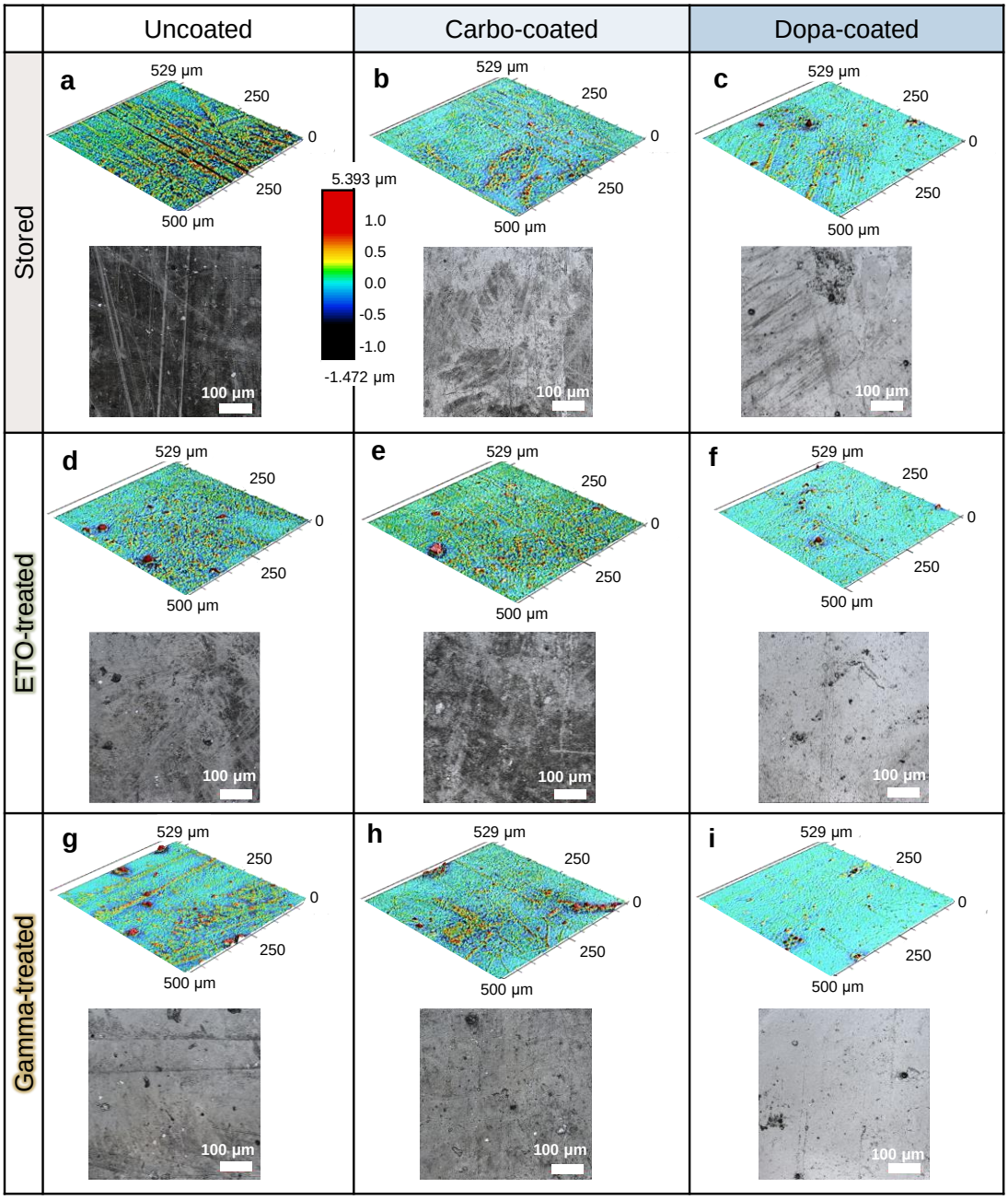

Figure SI 4: *Surface morphologies and laser microscopy images of coated and sterilized samples:* For each coating/treatment combination, a representative set of images (taken with 20x magnification) of the resulting surface structure is displayed; colored images represent height-scaled 3D surface morphologies (top pictures); grey-scale images represent laser microscopy image (bottom pictures). The color scale located between subfigures a) and b) applies to all images depicting surface morphologies.

142

SI 5 FTIR scans of sterilized samples

To examine putative influences of the sterilization processes on the substrate material or coating composition, FTIR scans were conducted as described in **SI 1**. In **Figure SI 5,** the spectra obtained for stored (uncoated or coated) samples are compared to spectra determined for samples subjected to a sterilization treatment.

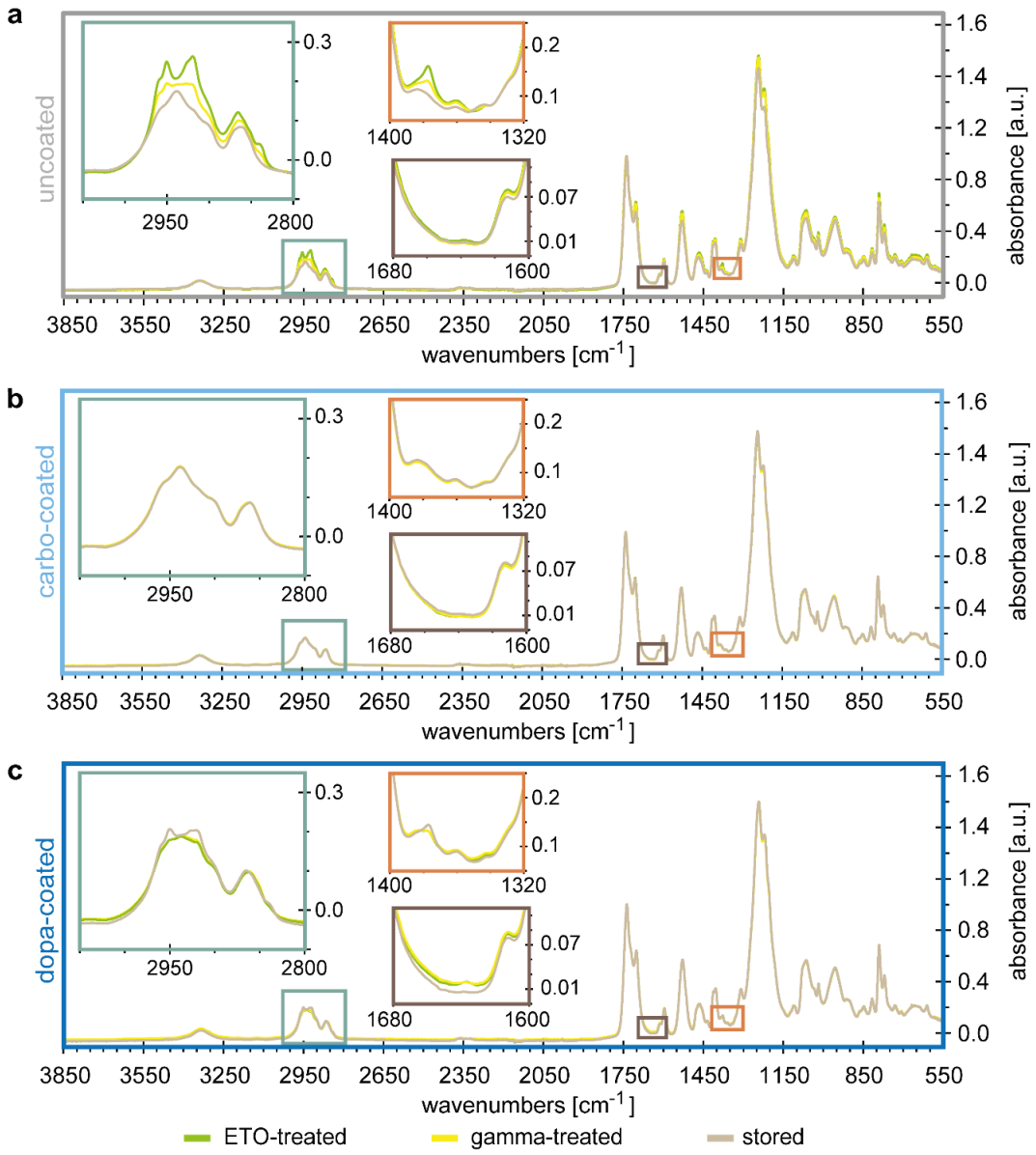

Figure SI 5: *FTIR spectra of different foil samples:* spectra are shown for a) uncoated, b) carbo-coated, and c) dopa-coated samples which were treated with either ethylene oxide fumigation (ETO, green) or γ-irradiation (gamma, yellow), or simply stored in a dry state (stored, beige). The legend at the bottom of the figure applies to all subfigures.

When using the stored samples as a reference, for each sterilization treatment, the changes caused by the sterilization process can be studied. For the uncoated samples, there is a strong change in the abundance of aliphatic C-H stretching vibrations in the 3000-2800 cm^{-1} range and in the vibrations around 1377 cm^{-1}. The ETO-treatment seems to trigger the appearance of two strong peaks indicating CH_3 and CH_2 asymmetric stretching. These peaks are similar to the bands we notice for the unsterilized dopa-coated sample in **Figure SI 1**; for uncoated samples, those must originate from the ethylene oxide fumigation. The simplest explanation would be that the observed bands are caused by hydrogen bonding of residual ethylene oxide molecules.

For carbo-coated samples, we detect no noticeable change in the FTIR spectra upon either sterilization treatment. It is, however, not fully clear why this is the case. Potentially, a change in the surface properties caused by the plasma treatment (@ 60 W for 25 min), removal of lighter aliphatic species upon exposure to highly concentrated solvents (*e.g.*, 96 % ethanol for 1 h), or the presence of the dextran layer on the surface could have rendered the foils more resistant to alterations by sterilization. In any case, the result indicates that the carbo-coated samples exhibit an increased inertness toward the two sterilization methods than uncoated foils.

For the dopa-coated sample, both sterilization treatments reduction the abundance of the CH_2 and CH_3 asymmetric stretch at 2920 cm^{-1} and 2950 cm^{-1}, as well as the 1377 cm^{-1} CH_3 peak. This result could indicate a change in the coating or of selected exposed groups from the coating; however, without spectral changes outside the aliphatic C-H vibrations, it is difficult to make a more detailed assessment.

Overall, both coatings appear to provide the foils with improved resistance towards the two sterilization treatments tested here – with the carbo-coated samples experiencing basically no change and the dopa-coated samples only minor changes compared to the uncoated samples. However, to fully assess and understand the origin of this enhanced resilience introduced by the coatings, further studies would be needed.

SI 6 References

[1] SpectraBase, Dopamine hydrochloride: Attenuated Total Reflectance Infrared (ATR-IR) Spectrum. https://spectrabase.com/spectrum/9HdJ7pFzgn1 (accessed July 18th, 2023).

[2] SpectraBase, N1-[3-(Trimethoxysilyl)propyl]-1,2-ethanediamine: Attenuated Total Reflectance Infrared (ATR-IR) Spectrum. https://spectrabase.com/spectrum/KB8BLkV1YdM (accessed July, 18th 2023).

[3] SpectraBase, Dextran: Attenuated Total Reflectance Infrared (ATR-IR) Spectrum. https://spectrabase.com/spectrum/BDKq1MblXC4 (accessed July 18th 2023).

[4] IRUG, Dextran from Leuconostoc mesenteroides: Interactive IRUG Spectrum. http://www.irug.org/jcamp-details?id=7047 (accessed July 18zh 2023).

[5] SpectraBase, DL-lysine: Attenuated Total Reflectance Infrared (ATR-IR) Spectrum. https://spectrabase.com/spectrum/89KyMH3B2yR (accessed July 18th 2023).

[6] SpectraBase, Quarternary ammonium compound: Transmission Infrared (IR) Spectrum. https://spectrabase.com/spectrum/GIeuiZ5tVi6 (accessed July 18th 2023).

[7] Z. Chen, N. Hadjichristidis, X. Feng, Y. Gnanou, Poly(urethane–carbonate)s from Carbon Dioxide, Macromolecules 50 (2017) 2320–2328. https://doi.org/10.1021/acs.macromol.7b00142.

[8] ChemicalBook, N-[3-(Trimethoxysilyl)propyl]ethylenediamine. https://www.chemicalbook.com/ChemicalProductProperty_EN_CB3129690.htm (accessed July 24th 2023).